

Title no. 90-M47

Analysis of Chloride Diffusion into Partially Saturated Concrete



by Anna V. Sietta, Roberto V. Scotta and Renato V. Vitaliani

The governing equations of moisture, heat, and chloride-ion flows through concrete within the framework of a distributed parameter model are described. The coupling terms and the nonlinearity of the problem are taken into account and a numerical procedure based on the finite element method is developed to solve the set of equations. The aim of this study is to examine chloride diffusion even in partially saturated concrete by considering the variability of ion diffusion coefficients with concrete parameters. Chloride intrusion in various environmental conditions is investigated and the effect of moisture flux in transporting dissolved ions through the porous media is considered. Comparisons with experimental tests are also carried out to show the reliability and the effectiveness of the proposed numerical model.

Keywords: chlorides; concretes; durability; diffusivity; hydration; partially saturated concrete; water.

Degradation of plain and reinforced concrete buildings due to physical and chemical attack is a major topic in civil engineering. The commonly held view that concrete is a durable maintenance-free construction material has been challenged in recent years, and it has been shown that such phenomena as carbonation, sulfate and chloride attack, and steel corrosion may cause concrete performance to be lower than expected.

One of the main causes of deterioration of concrete structures can be ascribed to chloride-induced corrosion, caused by the rapid penetration of chloride ions into concrete. Chloride permeation is a complex phenomenon, involving various factors such as diffusion of chloride ions and movement of chlorides due to permeation of water into concrete. The latter process conveys a greater quantity of ions than does the pure diffusion process. The basic parameters that should be considered when studying chloride diffusion in concrete and the related risk of corrosion are essentially the diffusion characteristics of concrete (which depend on pore-size distribution) and the chloride-binding capacity^{1,2} of concrete (both chemical and physical).

Many previous investigators have attempted to predict chloride concentration in concrete, but the scope of these works have generally been limited to a particular problem, and employed broad simplifications. The complexity of the mathematical formulation of the chloride-diffusion phenomena, resulting from nonlinearity and strong coupling with

governing equations, usually makes it necessary to apply numerical methods.

This paper focuses on developing a numerical algorithm that could predict chloride ingress into concrete. The requirement imposed was that this algorithm account for material parameters (and their variability with time), environmental conditions, and the interaction between the diffusion chloride ions and the concrete material. The development of this numerical procedure required a preliminary study to collect and organize experimental data for better understanding of the relationships between the variables involved in the physico-chemical process.

RESEARCH SIGNIFICANCE

The numerical algorithm reported simulates, and thus forecasts, chloride penetration into concrete materials in both saturated and unsaturated conditions in various environments. This was achieved with a new approach that considers suitable boundary conditions and the effect of moisture flux in transporting dissolved ions.

BASIC HYPOTHESES AND MODEL DESCRIPTION State of chlorides in concrete

Chlorides are often present as contaminants of concrete mix ingredients and, until recently, were the principal constituent of most accelerating admixtures. Dissolved chloride ions also may penetrate unprotected hardened concrete in structures exposed to marine environments or to deicing salts. In the first case we speak of "internal chlorides," in the second, of "external chlorides." Chlorides in concrete may be present in a number of states:²

- Free, where they are dissolved in the pore solution.
- Chemically bound, where they chemically react with the hydration compounds of cement, particularly with C₃A, to form calcium chloroaluminate (known as Friedel salts).

ACI Materials Journal, V. 90, No. 5, September-October 1993.
Received May 12, 1992, and reviewed under Institute publication policies. Copyright © 1993, American Concrete Institute. All rights reserved, including the making of copies unless permission is obtained from the copyright proprietors. Pertinent discussion will be published in the July-August 1994 ACI Materials Journal if received by Apr. 1, 1994.

Anna V. Saetta is a PhD student in structural mechanics at the Department of Civil Engineering, University of Padova, Italy, where she also lectures. Her dissertation concerns the durability of concrete structures, with special emphasis on the diffusion phenomena of aggressive substances.

Roberto V. Scotta graduated with honors in Civil Engineering in 1992 from the University of Padova, where he is now a PhD student. His thesis concerns chloride diffusion in concrete structures and the numerical modeling of such phenomena. He was the principal investigator for the work reported here.

Renato V. Vitaliani is Associate Professor of Automatic Calculus of Structures in the Department of Civil Engineering at the University of Padova. His research interests are in modeling materials and structural behaviors using such numerical methods as the finite element method. He is author or coauthor of three books and more than 80 papers.

Table 1—Relationships between free and total chlorides (external chloride source)¹

Source of Cl ⁻ ions	Cl ⁻ concentration, kg/m ³	Relationship of free (F) and total (T) chlorides
Seawater	18.5	$F = 0.55 \times T$
NaCl	20.0	$F = 0.55 \times T$
NaCl	45.0	$F = 0.70 \times T$
NaCl	90.0	$F = 0.80 \times T$
CaCl ₂	20.0	$F = 0.35 \times T$
MgCl ₂	20.0	$F = 0.50 \times T$

- Physically bound: attracted to the pore surface by weak Van der Waals forces.
- In a chemisorbed state.

It is generally recognized that only the free chloride ions influence the degradation of reinforced concrete by causing corrosion of embedded steel. This process is called "pitting corrosion." Corrosive action of chloride ions is continuously opposed by the film-repairing action (i.e., passivation layer) of hydroxyls. Using a probabilistic model, Haussmann³ proved that corrosion can start only when the ratio of free chloride concentration to hydroxyl concentration exceeds the value 0.63 ($R = Cl/OH \cong 0.63$). This result was experimentally confirmed by Gouda.⁴ As a consequence, the chloride threshold value depends on the pH of the pore solution, i.e., on the cement type used, salt-diffusing type and, if present, on the contemporary carbonation reaction. Many researchers have tried to find relationships between bound and free chlorides.^{5,6} Experimental results show that cements containing pozzolanic materials are able to bind chloride more effectively than OPC cement and that the bound chloride ratio depends also on the type of cation associated to Cl⁻. By adding 1 percent by weight of Cl⁻ ions as NaCl to cement paste, Arya and Newmann¹ found that free chloride concentration in porous solution was about 12000 ppm; the same value, in the case of addition of CaCl₂, HCl, or MgCl₂, was variable between 7000 and 7500 ppm. Cation type influences binding capacity because it can modify pH values in concrete. For external chlorides, Tritthart's experiments⁷ showed that the amount of fixed ions increases with a decrease of the pH value of the diffusing solution.

However, it is generally believed that free chloride content is proportional to the total chloride concentration. For external chloride, Arya and Newmann¹ found that there are linear relationships between these two quantities; the proportionality coefficients depend on diffusing solution type and on its concentration (Table 1). Linear proportionality is verified especially for chloride of external origin, the chemically bound chloride amount being negligible, while physically bound chlorides are in dynamic balance with that dissolved in the porous solution.

Chloride diffusion laws into saturated and unsaturated concrete

Ion diffusion in porous media is governed by Fick's first law

$$J_{Cl} = -D_i \cdot \nabla (C_f) \quad (1)$$

where J_{Cl} is the ion flux through a unitary area in a unit of time, kg/(m²·sec); C_f is the solution concentration, kg/m³; and D_i is the "intrinsic diffusion coefficient," m²/sec. The equation of chloride mass conservation (i.e., Fick's second law) is

$$\frac{\partial C_t}{\partial t} = \text{div} (J_{Cl}) \quad (2)$$

where C_t is the total chloride concentration in the unitary volume of the porous body, kg/m³. Replacing Eq. (2) into Eq. (1), we obtain

$$\frac{\partial C_t}{\partial t} = -\text{div} [D_i \cdot \nabla (C_f)] \quad (3)$$

If we prefer working in terms of total concentration C_t , Eq. (3) must be modified. In a saturated concrete we can write

$$C_t = w_{sat} \cdot C_f + (1 - w_{sat}) \cdot C_s \quad (4)$$

i.e., the total chloride concentration C_t is a weighted average of free chloride concentration and the chloride concentration in the solid volume C_s , kg/m³. w_{sat} represents the evaporable water content: it is often used to measure concrete porosity.⁸ If γ is the volumetric distribution coefficient of the species between the solid and the liquid

$$C_s = \gamma \cdot C_f \quad (5)$$

we can write

$$C_t = w_{sat} \cdot C_f + (1 - w_{sat}) \cdot \gamma \cdot C_f = \alpha \cdot C_f \quad (6)$$

where

$$\alpha = w_{sat} + (1 - w_{sat}) \cdot \gamma \quad (7)$$

where α is the capacity factor, which can be regarded as a measure of the binding capacity of the saturated porous media for a particular diffusant. The range of parameter α was investigated by Atkinson and Nickerson⁹ for I^- and Cs^+ ions; they found values generally variable from 0.5 to 1. The α value depends on concrete porosity (and therefore on water-cement ratio) and coefficient γ , which measures chloride binding. Consequently

$$\frac{\partial C_t}{\partial t} = -\text{div} [D_a \cdot \nabla (C_f)] \quad (8)$$

where $D_a = D_i / \alpha$ is the apparent diffusion coefficient that is influenced by adsorption phenomena. When concrete is in unsaturated conditions, Eq. (4) must be corrected to take into account that the concrete porosity is partially water filled. Retaining Eq. (5) as still true, we obtain

$$\alpha = w + (1 - w_{sat}) \cdot \chi \quad (9)$$

where w is the effective water content, m^3/m^3 , which is always less than w_{sat} . Note the difference between D_i and D_a , which are, respectively, the intrinsic and apparent diffusion coefficients: the latter is associated with a total chloride concentration gradient averaged in the whole volume of porous medium, while D_i is relative to the concentration gradient of free dissolved chlorides.

The analytical integration of Eq. (8) is simply obtained only in the following conditions:

- monodimensional problem on a semi-infinite body
- apparent diffusion coefficient D_a constant in space and in time
- boundary conditions C_{en} constant for $t > 0$.

With these assumptions, it is possible to obtain a linear solution that could be applied in a simplified assessment of chloride diffusion, but this is not able to describe the general conditions existing in nature. Temperature, relative humidity, and cement hydration evolution cause variability of D_a in both time and space. Moreover, except in the case of continuous immersion of concrete in a salt solution with a constant concentration, the condition of C_{en} constant is unattainable. If we want to consider these effects, Eq. (8) must be numerically integrated and the dependence of D_a on the internal material parameters defined.

Variability of D_a with relative humidity, cement hydration degree, and temperature

Available experimental results¹⁰⁻¹⁵ show that chloride rate entry depends on temperature, concrete porosity, cement type, cation type associated to Cl^- ions, and curing conditions. Porosity is a direct function of water-cement ratio (w/c): when the ratio increases the diffusion characteristic increases more than proportionally. In OPC concrete, Collepardi¹¹ found that when porosity increases from 11.4 percent ($w/c = 0.5$) to 13.4 percent ($w/c = 0.6$) D_a values increase from 1.7 to $3.3 \cdot 10^{-12}$ m^2/sec . In OPC paste with $w/c = 0.4, 0.5,$ and 0.6 , Page¹² measured, respectively, $D_a = 2.6, 4.47,$ and $12.5 \cdot 10^{-12}$ m^2/sec .

Table 2—Diffusion activation energies U in various cement pastes^{12,15}

w/c	U, KJ/mol	
	Ordinary portland cement	Pozzolan cement
0.4	41.8 ± 4.0	—
0.5	44.6 ± 4.3	4.18
0.6	32.0 ± 2.4	—

Pozzolanic cement generally shows diffusivity characteristics smaller than OPC. In OPC paste made with water-cement ratio of 0.5, Byfors¹³ found $D_i = 6.8 \cdot 10^{-12}$ m^2/sec ; when 20 percent of the cement was substituted with silica fume, D_i became $0.59 \cdot 10^{-12}$ m^2/sec ; when 15 percent of cement was replaced by fly ash it became $3.2 \cdot 10^{-12}$ m^2/sec . In investigating the effect of associated cations, Collepardi¹⁰ proved that the diffusivity of Cl^- added as KCl is about three-fourths of that of the same ion added as $CaCl_2$.

Detwiler et al.¹⁴ asserted that accelerated concrete maturation at 50 C leads to double diffusion coefficients. From all the available experimental data listed in the literature, we can define a reference value of the intrinsic diffusion coefficient which takes into account all of the variables listed. This $D_{i,ref}$ was evaluated in standard conditions of temperature ($T_0 = 23$ C), relative humidity ($h = 100$ percent) and cement hydration degree (e.g., after 28 maturation days in standard conditions). This reference value was then corrected to consider the effective values assumed by these three parameters (which are variable both in time and in space during numerical simulation). The following relationship can be used

$$D_i = D_{i,ref} \cdot f_1(T) \cdot f_2(t_e) \cdot f_3(h) \quad (10)$$

where $f_1(T)$ takes into account the dependence of coefficient D_i on the temperature T ; according to the Arrhenius' law

$$f_1(T) = \exp \left[\frac{U}{R} \cdot \left(\frac{1}{T_0} - \frac{1}{T} \right) \right] \quad (11)$$

in which T and T_0 are expressed in deg K ($T_0 = 296$ K is the reference temperature), R is the gas constant [KJ/(mol·K)] and U is the activation energy of the diffusion process, KJ/mol. Page¹² and Collepardi¹⁵ found that U is dependent on porosity and on cement type, as shown in Table 2.

Chloride diffusivity in concrete decreases with an increase of cement hydration degree and trends asymptotely to a final value when maturation nears completion. As proposed by Bazant,¹⁶ hydration degree can be taken into account by introducing the "equivalent maturation time" t_e defined by

$$t_e = t_{e,in} + \int_0^t \beta_h \cdot \beta_T \cdot dt \quad (12)$$

with

experimental results^{17,18} was obtained using an S-shaped curve that can be expressed by the following relationship

$$f_3(h) = \left[1 + \frac{(1-h)^4}{(1-h_c)^4} \right]^{-1} \quad (16)$$

In Eq. (16) h_c characterizes the humidity at which the coefficient D_i drops halfway between its maximum and minimum values. To define this law, we have also considered the analogy that exists between chloride and water diffusion in unsaturated concrete. This latter phenomenon was reproduced by Bazant¹⁶ by a relationship similar to Eq. (16).

Chloride transport in water flux

When the porous media is subjected to drying and wetting cycles the movement of water into the pores is intense and therefore the application of the only concentrated diffusion concept seems inadequate if the permeation phenomenon of chloride is to be clarified.¹⁸ In this case a certain amount of chlorides in solution is dragged by water flux and this causes a further term to be added to the diffusion process. By considering an element of infinitesimal dimension dx , dy , and dz of porous media crossed by a moisture flux $J_w = (J_{w,x}; J_{w,y}; J_{w,z})$, the chloride mass conservation imposes that the total chloride content variation is equal to the difference between the entering chloride flux and the exiting one

$$\begin{aligned} \frac{dQ_{Cl}}{dt} &= \frac{dC_t}{dt} \cdot dx \cdot dy \cdot dz \\ &= [J_{C,x}(x) - J_{C,x}(x+dx)] dy \cdot dz \\ &\quad + [J_{C,y}(y) - J_{C,y}(y+dy)] dx \cdot dz \\ &\quad + [J_{C,z}(z) - J_{C,z}(z+dz)] dx \cdot dy \end{aligned} \quad (17)$$

The chloride flux J_C due to water flux can be written as the product of the moisture flux J_w and the free chloride concentration C_f in solution

$$J_C = C_f \cdot J_w \quad (18)$$

with the simplification that C_f can be assumed constant within a small region of material. J_w is expressible in Fourier's series as follows

$$J_w(x+dx) \approx J_w(x) + \frac{\partial J_w(x)}{\partial x} \cdot dx \quad (19)$$

By substituting Eq. (18) and (19) into Eq. (17) we obtain

$$\frac{\partial C_t}{\partial t} = -C_f \cdot \text{div}(J_w) = \frac{C_t}{\alpha} \cdot \frac{\partial w}{\partial t} \quad (20)$$

where $\partial C_t / \partial t$ represents the variation in time of the total chloride concentration due to the transport mechanism only. Eq. (20) is part of the total diffusion process and must be included so that the mass is conserved. Thus we obtain the following global relation used in a numerical algorithm

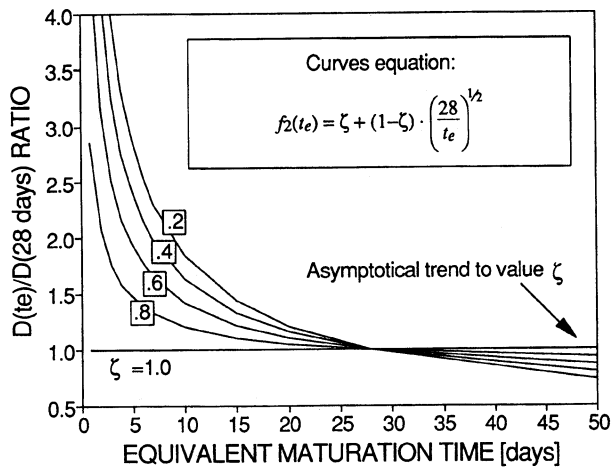


Fig. 1—Decrease of chloride diffusion coefficient due to increase of equivalent maturation time t_e for different values of parameter ζ

$$\beta_h = \left[1 + (3.5 - 3.5 \cdot h)^4 \right]^{-1} \quad (13)$$

$$\beta_T = \exp \left[\frac{U}{R} \cdot \left(\frac{1}{T_0} - \frac{1}{T} \right) \right] \quad (14)$$

in which $U/R = 2700$ deg K and $T_0 = 296$ deg K.

To consider the decrease of the diffusivity with the increase of the hydration degree, we developed the following equation

$$f_2(t_e) = \zeta + (1 - \zeta) \cdot \left(\frac{28}{t_e} \right)^{1/2} \quad (15)$$

with t_e in days. Coefficient ζ is variable from 0 to 1; it is the ratio between the diffusion coefficient for $t_e \rightarrow \infty$ and the diffusion coefficient for $t_e = 28$ days. The range of its variation is from 0 to 1. This parameter measures how much the diffusivity decreases with time. By varying ζ we obtain the curves shown in Fig. 1. For concretes with low w/c and a rapid-hardening cement (which reaches low diffusion coefficient after a few days of hydration) the parameter ζ can be assumed to be near 1; for concretes made with higher w/c , ratio ζ is lower, because D_i decreases with t_e at a more rapid rate.

To analyze the ion diffusion in partially saturated media, it is necessary to derive the relationship between D_i and the relative humidity h in concrete. The ion diffusion is a humid process, which can occur only if water is present in the pores. In saturated conditions, ions can diffuse through the continuously water-filled channels; when the water content decreases, the diffusion process is hindered by the decrease of the number of porous channels, which have a continuity of pore solution, and because of the strong rise of the interaction forces between cement paste and ions due to the decrease of the thickness of the adsorbed water layers. When the relative humidity h drops below the critical value $h_c = 75$ percent, the ion diffusivity shows a rough drop. The best fit with

$$\frac{\partial C_t}{\partial t} = -\text{div}[D_a \cdot \nabla(C_t)] + \frac{C_t}{\alpha} \cdot \frac{\partial w}{\partial t} \quad (21)$$

Coupling with humidity and heat diffusion

The chloride diffusion mechanism in concrete is strictly linked with coupled diffusion of relative humidity (taken as the parameter determining water content in concrete) and heat. It was seen previously that the diffusion coefficient D_i (or D_a) is strongly influenced by h and T values and that the movement of water causes ion transport. To predict the evolution of the cement hydration it is also necessary to predict humidity and temperature levels.

The moisture and heat flows through concrete are governed by the following relationships proposed by Bazant^{16,19}

$$\rho \cdot C \cdot \frac{\partial T}{\partial t} = \text{div}[\lambda \cdot \nabla(T)] \quad (22)$$

$$\frac{\partial h}{\partial t} = -\text{div}[D_h(h, T, t_e) \cdot \nabla(h)] + \frac{dh_s}{dt} + K \cdot \frac{dT}{dt} \quad (23)$$

where ρ is the concrete specific mass, kg/m^3 ; C is the concrete specific heat capacity, $\text{J}/(\text{kg} \cdot \text{deg C})$; λ is the thermal conductivity, $\text{W}/(\text{m} \cdot \text{deg C})$; D_h is the humidity diffusion coefficient, m^2/sec ; dh_s/dt is the relative humidity variation due to self-desiccation; and $K \cdot dT/dt$ is the coupling term with heat diffusion.

For the sake of simplicity in the heat diffusion equation the parameters ρ , C , and λ were assumed constant; instead, the humidity diffusion is nonlinear. Correlation between the relative humidity and the free water content is assured by sorption and desorption isotherms, expressed by

$$w = w_{\text{sat}} \cdot h \quad \text{desorption} \quad (24)$$

$$w = w_{\text{sat}} \cdot h \cdot (1.16 \cdot h^3 - 1.05 \cdot h^2 - 0.11 \cdot h + 1) \quad \text{sorption} \quad (25)$$

The sorption isotherm relationship was used by Bazant¹⁹ while the desorption isotherm equation reproduces, in the absence of sure experimental data, the shape supposed by many researchers.²⁰ Both isotherms do not consider hydration effects.

Boundary conditions

In first approximation, the humidity flux from the concrete surface to the external environment (or vice versa) can be assumed linearly dependent on the difference between the relative humidity in surface layer h and the environmental humidity h_{en} ¹⁹

$$\underline{n} \times \underline{J}_h = B_h \cdot (h - h_{en}) \quad (26)$$

with B_h = surface mass transfer coefficient, $1/(\text{m}^2 \cdot \text{sec})$; $\underline{n} \times \underline{J}_h$ = scalar product of \underline{n} , versor normal to surface; and \underline{J}_h = humidity flux, $1/(\text{m}^2 \cdot \text{sec})$. This assumption lets us simulate

a perfectly sealed surface ($\underline{J}_h = 0$) by assuming $B_h = 0$ and the condition of perfect superficial transmission by assuming $B_h \rightarrow \infty$. Similarly, heat flux \underline{q} normal to the surface is the product between B_T [surface heat transfer coefficient, $\text{W}/(\text{m}^2 \cdot \text{C})$] and the difference between the superficial temperature T and the environmental temperature T_e ¹⁹

$$\underline{n} \times \underline{q}_h = B_T \cdot (T - T_{en}) \quad (27)$$

For greater accuracy, the surface thermal exchange should depend on the fourth power of the temperature difference: this was not considered for the sake of operative simplicity.

According to Bazant's assertion,¹⁹ the better fit of the numerical results with the experimental data obtained by drying tests of concrete specimens has been reached by assuming the value of B_T in the range 0.05 to 0.1, $(\text{m}^2 \cdot \text{sec})^{-1}$, and with the value of B_h approaching infinite (this occurs also because the rate of evaporation is often much faster than the rate of humidity change inside the specimen). Consequently, in all the numerical examples we have used

$$B_T = 0.07 (\text{m}^2 \cdot \text{sec})^{-1}$$

$$B_h = 1.0 (\text{m}^2 \cdot \text{sec})^{-1}$$

Ideally, the environmental conditions determining chloride diffusion into concrete structures can be distinguished in two classes characterized by the relations reproducing the different boundary conditions. The first type of boundary condition is to give the chloride concentration in aqueous solution in contact with the concrete surface; it is the case of exposure by immersion, continuous or discontinuous, of the concretes in marine water or the case of the laboratory specimens immersed in salt solutions of constant concentration. If C_{en} is the concentration of the external solution, the chloride flux crossing the surface thickness in a unit of time and through a unitary area can be described as follows

$$\underline{n} \times \underline{J}_c = B_c \cdot (C_f - C_{en}) + C_{en} \cdot \underline{n} \cdot \underline{J}_w \quad (28)$$

where $\underline{n} \times \underline{J}_c$ is the chloride flux normal to the surface, $\text{kg}/(\text{m}^2 \cdot \text{sec})$; B_c is the surface chloride transfer coefficient, m/sec ; and the second term in the right-hand side represents the contribution of the entering water flux in chloride transport (this term was imposed equal to zero in drying phases because when the water goes out of the concrete, it evaporates, leaving on the surface the dissolved salts).

Similar to the surface mass and heat transfer coefficients B_h and B_T , the surface chloride transfer coefficient B_c must be quantified by fitting experimental data. The agreement was satisfactory for B_c varying between 1 and 6 m/sec . However, we have found that significant variations of B_c have a negligible influence on the final result. In fact, in case of saturated concrete immersed in chloride aqueous solution, during only the initial phase of the test, the chloride diffusion phenomenon is influenced by the surface chloride transfer coefficient, while the long-time results are only related to

the value of the diffusion coefficient D_a of the concrete material.

The second type of boundary condition simulates the building's exposure to the marine atmospheres. In these environments, chlorides are transported by wind to the concrete surface in the form of small drops of seawater. The ion concentration in the superficial layer of concrete is controlled by the deposition process of the chlorides present in the air and by the contrasting washing effect of rain. The amount of ions deposited or washed in a unitary time and for a unitary area is given by the following relationship

$$\frac{dQC}{dt} = k_{dep} \cdot C_{atm} - k_{dil} \cdot C_t \quad (29)$$

where $k_{dep} \cdot C_{atm}$ is the ion deposition rate, $\text{kg}/(\text{m}^2 \cdot \text{sec})$; C_{atm} is the ion concentration in atmosphere, kg/m^3 ; k_{dep} is the deposition coefficient, m/sec ; $k_{dil} \cdot C_t$ is the washing away rate, $\text{kg}/(\text{m}^2 \cdot \text{sec})$; C_t is the total chloride concentration, kg/m^3 ; and k_{dil} is the washing-away coefficient, m/sec . Deposition rate decreases if the distance from sea coast increases or if the concrete porosity decreases. A similar relationship was used by Masuda²¹ in his studies.

For the partially saturated concrete, the deposition coefficient k_{dep} and the washing-away coefficient k_{dil} must be chosen by a careful fitting of many experimental data. For this study, only a few experiments were available, which limited identification of the k_{dep} and k_{dil} values only for particular cases. However, we expect that if sufficient data were available from controlled tests on concrete specimens, these coefficients could be precisely selected for whatever environmental conditions and for each type of concrete.

FINITE ELEMENT FORMULATION

For the sake of simplicity, only one-dimensional problems are analyzed. Moreover, because Eq. (23), (24), and (25) have a similar structure, our interest is reserved only for Eq. (23), which is more pertinent to the arguments discussed in this paper.

To formulate a finite element scheme, we may apply a standard residual procedure^{22,23}

$$\int_e w_i \cdot \left[\frac{\partial C_t}{\partial t} + \frac{\partial}{\partial x} \cdot \left(D_a \cdot \frac{\partial C_t}{\partial x} \right) - \frac{C_t}{\alpha} \cdot \frac{dw}{dt} \right] \cdot dx = 0 \quad (30)$$

Introducing finite element approximation with the interpolation functions N_i (of the i th element) and choosing a standard Galerkin method (i.e., $w_i = N_i$), we have

$$C(x,t) = \sum N_i(x) \cdot C_i(t) \quad (31)$$

and

$$\int_e N^T \cdot \left[N \cdot \frac{\partial C_t}{\partial t} + \frac{\partial}{\partial x} \left(D_a \cdot \frac{\partial}{\partial x} \cdot N \cdot C_t \right) - N \cdot \frac{dw}{dt} \cdot \frac{1}{\alpha} \cdot N \cdot C_t \right] \cdot dx = 0 \quad (32)$$

We integrate by parts to get rid of the second spatial derivatives of C_t and at the same time to eliminate derivatives from the boundary terms in Eq. (32).

$$\int_e N^T \cdot N \cdot dx \cdot \frac{\partial C_t}{\partial t} + (N^T \cdot D_a \cdot N \cdot C_t)_{x=0}^{x=l} + \left[\int_e \left(B^T \cdot D_a \cdot B + N^T \cdot N \cdot \frac{dw}{dt} \cdot \frac{1}{\alpha} \cdot N \right) dx \right] C_t = 0 \quad (33)$$

The latter equation can be rewritten in the following form

$$V \cdot \frac{\partial C_t}{\partial t} + (K + K') \cdot C = q \quad (34)$$

where

$$V = \int_e N^T \cdot N \cdot dx; \quad K = \int_e B^T \cdot D_a \cdot B \cdot dx; \\ K' = \int_e N^T \cdot N \cdot \frac{dw}{dt} \cdot \frac{1}{\alpha} \cdot N \cdot dx \quad (35)$$

and q is the vector of the external forces given by the integration of the boundary conditions.

The matrix differential Eq. (34) may be integrated in time by a step-by-step procedure, applying a general trapezoidal algorithm. To this end, we introduce discrete time steps $\Delta t = t_{n+1} - t_n$ ($n = 1, 2, \dots$) and we obtain

$$\left[V^{n+1} + \omega \cdot \Delta t \cdot (K + K')^{n+1} \right] C_t^{n+1} \\ = \left[V^n + (1 - \omega) \cdot \Delta t \cdot (K + K')^{n+1} \right] C_t^n \\ + \Delta t \cdot [\omega \cdot q^{n+1} + (1 - \omega) \cdot q^n] \quad (36)$$

where the superscript n indicates that the terms are calculated at step n . This equation contains the whole family of the trapezoidal scheme: when $\omega = 0.5$ we have the Crank-Nicholson method; when $\omega = 1$ we have the forward difference method; and when $\omega = 0$ we have the backward difference method. It is worthwhile to note that when $0.5 < \omega < 1$, the resulting methods are unconditionally stable. In our tests we generally used $\omega = 0.8$.

For the numeric solution of the equations system we used an iterative procedure. If, at time step n , the solution vectors h^n , T^n and C_t^n are known and we want to estimate the same vectors at time step $n + 1$, the following steps must be carried out:

a. Solution of heat diffusion equation, which is, in our formulation, a linear problem independent of humidity and chloride diffusion.

b. Solution of the nonlinear equation describing the humidity diffusion phenomenon. The solution is dependent on T^{n+1} , which is known. The nonlinearity of the problem is included into the dependence of D_h upon unknown h^{n+1} and the solution is reached by using a modified Newton-Raphson

Table 3—Values of the parameters used in numerical simulation of chloride diffusion in saturated concrete

Concrete type	Diffusion coefficient $D_{a,rif}$, m^2/s		ζ
	3 days	28 days	
w/c = 0.32	$1.75 \cdot 10^{-13}$	$0.59 \cdot 10^{-13}$	0.8
w/c = 0.44	$2.60 \cdot 10^{-12}$	$1.57 \cdot 10^{-12}$	0.6
w/c = 0.55	$1.90 \cdot 10^{-11}$	$1.46 \cdot 10^{-11}$	0.5

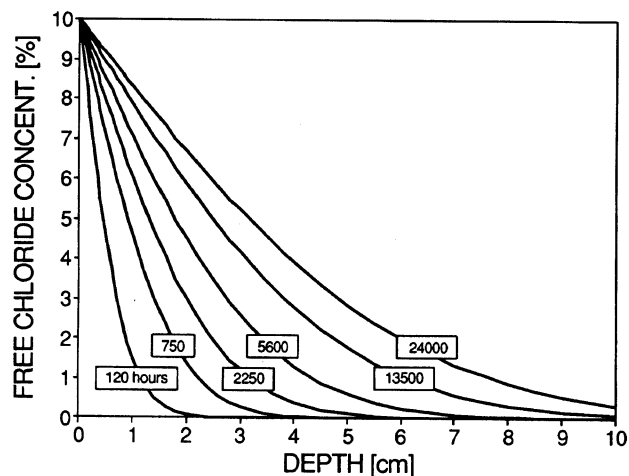


Fig. 2—Diffusion kinetic of chloride ions into OPC concrete, w/c = 0.55; aged 3 days before immersion in a 10 percent CaCl₂ solution

algorithm in which the matrixes are recalculated at a fixed number of iterations.

c. At least C^{n+1} is given by solution of Eq. (36) by using the knowledge of T^{n+1} and w^{n+1} .

NUMERICAL APPLICATIONS

Chloride ion diffusion in permanently saturated concrete

The following numerical example reproduces the Cl⁻ ion penetration into the concrete specimens immersed into a 10 percent CaCl₂ aqueous solution. It fits the penetration depths measured by Collepardi²⁴ in his laboratory tests. The specimens were cast with OPC concrete, w/c = 0.32, 0.44, and 0.55, and they aged 3 or 28 days in standard conditions before exposure to CaCl₂ solution. It was thus possible to show how the w/c and the curing period can influence the chloride penetration rate. The parameters used in numerical simulation are summarized in Table 3 and the simulated exposition time was 1000 days long. The test conditions imposed were $h = 100$ percent, $T = 23$ C, and the external solution $C_{en} = 10$ percent Cl⁻ (constant). The numerical analysis gives the results represented in Fig. 2 through 4. Chloride penetration depths are characterized by reaching the total concentration level of 0.07 percent Cl⁻. This is approximately the value marking the chloride penetration front in Collepardi's measurements, which were carried out by spraying fluoresceine on the split specimen surfaces. Note the good agreement between numerical and experimental penetration curves. In-

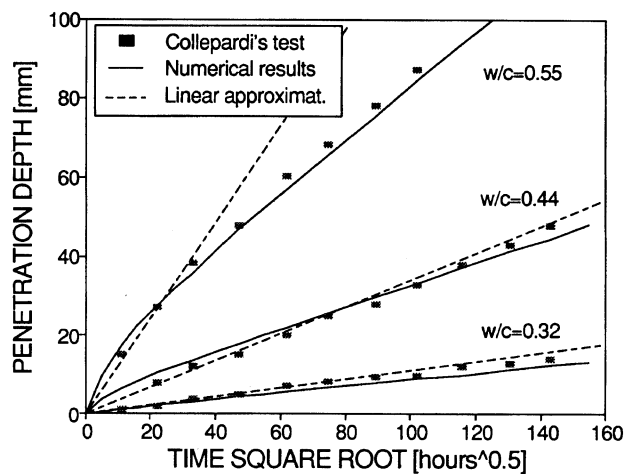


Fig. 3—Comparison of chloride penetration depths versus immersion time; OPC concrete specimens immersed in 10 percent CaCl₂ aqueous solution, cured 3 days

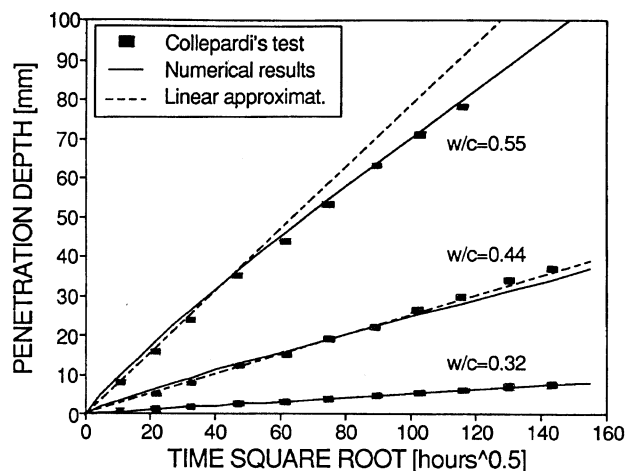


Fig. 4—Comparison of chloride penetration depths versus immersion time; OPC concrete specimens immersed in 10 percent CaCl₂ aqueous solution, cured 28 days

adequacy of the linear dependence of the ions' penetration on time square root in forecasting chloride diffusion in young concrete, especially if made with high w/c ratio, is also evident from Fig. 3 and 4.

As expected, independent of the curing time, the chloride penetration depth increases with the w/c, i.e., with the increase of the diffusion coefficient, and this fact is more evident for the higher diffusion coefficients. Also the effect of the curing time on the chloride penetration can be pointed out by comparing Fig. 3 with Fig. 4—the shorter the curing time, the faster the chloride penetration.

In this example, various attempts were performed to establish how much the variability of the chloride transfer coefficient B_C could modify the final results, and it was observed that the total chloride content shows no significant variation also for very different values of B_C (see Fig. 2).

Chloride diffusion in unsaturated concrete

The exposure condition of building facades to a marine atmosphere (near the sea coast), was reproduced in this example. The boundary conditions used in reproducing the

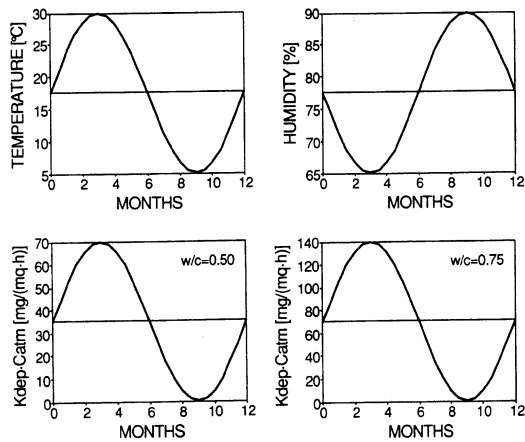


Fig. 5—Seasonal variability of daily average values of temperature, humidity, and superficial deposition rate of chloride used to study chloride intrusion into concretes exposed to sea atmosphere

Table 4—Values of parameters used in numerical simulation of chloride diffusion in unsaturated concretes

Quantity	Concrete type	
	w/c = 0.5	w/c = 0.75
ζ	0.7	
Heat diffusion		
λ , W/(m · deg C)	0.001	
$\rho \cdot C$, J/(m ³ · deg C)	$1.936 \cdot 10^{+06}$	
Initial temperature T_i , C	20	
Humidity diffusion		
Porosity, %	11	14
D_h , m ² /s	$3.0 \cdot 10^{-11}$	$1.0 \cdot 10^{-10}$
Initial humidity h_i , %	90	
Chloride diffusion		
Binding ratio γ	0.7	
V/R	deg K	3000
k_{dl} , m/sec	$5.0 \cdot 10^{-10}$	
$D_{i,rif}$, m ² /sec	$3.0 \cdot 10^{-11}$	$0.5 \cdot 10^{-11}$
Initial chloride concentration $C_{t,i}$, kg/m ³	0	

chloride diffusion were imposed by using Eq. (29). To make the numerical test more significant, we considered a sinusoidal variability in time of the environmental parameters h_{en} , T_{en} , and C_{en} within a 1-yr period (Fig. 5); this assumption reproduces the seasonal variation of the daily average values of the three parameters. The numerical simulation covered a 39-month period, the beginning of which coincided with the early summer phase. Two different types of concrete, one with $w/c = 0.5$ and the other with $w/c = 0.7$, were considered and were characterized by the quantities summarized in Table

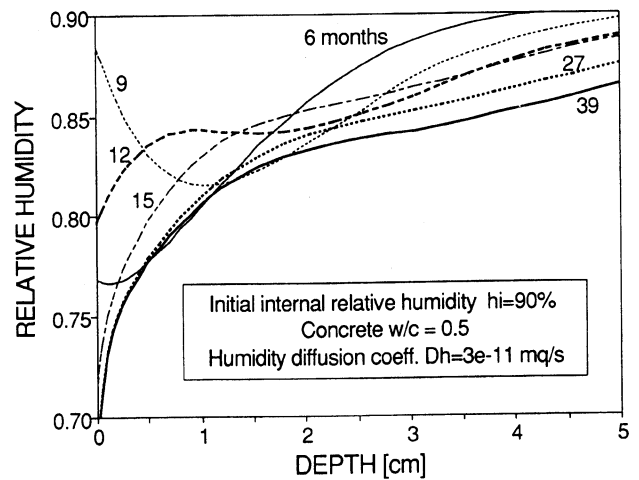


Fig. 6—Curves representing relative humidity for different exposure periods in concrete with $w/c = 0.5$

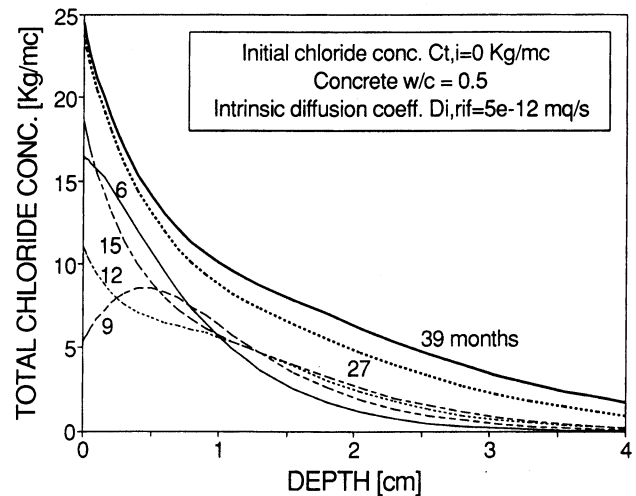


Fig. 7—Curves representing total chloride concentration for different exposure periods in concrete with $w/c = 0.5$

4. The chloride deposition rate k_{dep} was assumed double for concrete of $w/c = 0.75$, because the greater porosity favors chloride deposition.

In the resulting Fig. 6 and 7, the variability of the h and C_t profiles in the superficial thickness can be observed. Fig. 8 and 9 show the total chloride concentration obtained, respectively, at the end of the winter and the summer periods into two different concretes. The decreased deposition speed during the winter period induces a drop of the total chloride concentration in external layers leading to the formation of particular peaks of the curves near the surface during this season (Fig. 8). This typical shape was observed by Jaegermann²⁵ in concrete specimens exposed to marine atmosphere at 30 m from the sea coast after a 3-year-long exposure period. Note that the chloride concentration peaks are more pronounced and nearer to the surface in the concrete with $w/c = 0.5$. In fact, a lesser D_i value causes chloride accumulation in the superficial layer, where the ions can be easily washed away by rainfall. However, the lower the w/c , the more

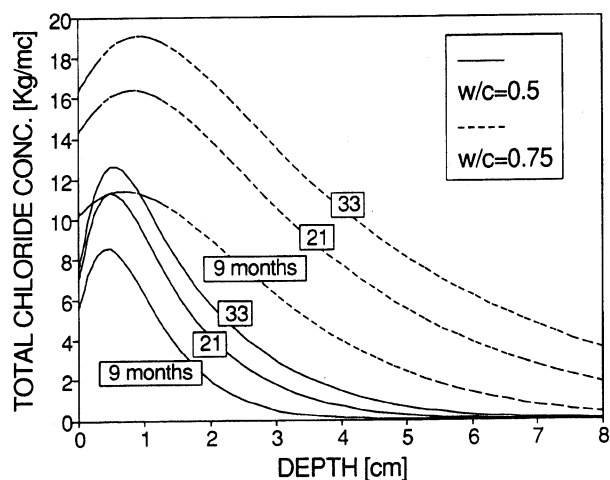


Fig 8—Profiles of total chloride concentration for two concretes at the end of winter exposure

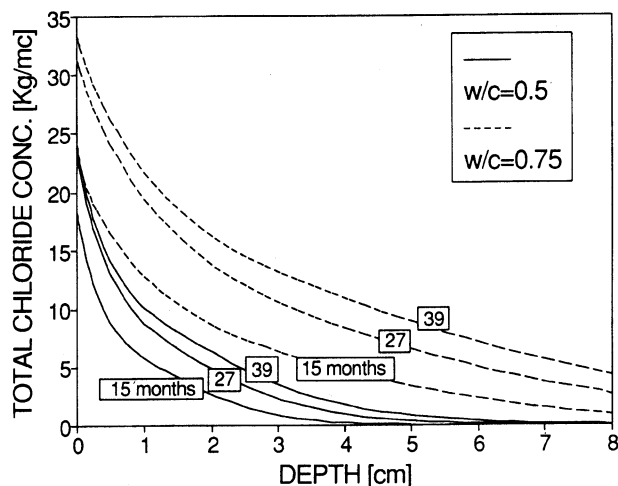


Fig. 9—Profiles of total chloride concentration for two concretes at the end of summer exposure

difficult the chloride penetration in concrete, as shown in Fig. 8 and 9.

In this example, only the effect of the deposition coefficient k_{dep} has been considered. Its value was increased with porosity, to simulate the actual growth of the chloride deposition. The value of the washing-away coefficient k_{dil} has been kept at a constant value, which is representative of the concretes and the environmental conditions considered. The range of k_{dil} and k_{dep} values, which could be precisely identified within the limited time scale of the research reported in this paper, will be easily extended as soon as enough experimental data is available.

Chloride intrusion by drying-wetting cycles

This test examined the kinetic of chloride penetration mainly due to the water flux. One of the most significant examples of this process is the ion intrusion into concrete exposed in a tidal zone, that is alternatively wetted by sea water and dried by air and sun. Experimental investigations on off-shore structures made by Uji, Matsuoka and Maruya²⁶ showed that the total chlorides content in superficial thickness was about 0.360 percent by weight of concrete after 7 years exposure and became 0.85 percent after 60 years on average. The theoretical surface chloride contents, when pores at the concrete surface are assumed to be filled with the seawater or with the saturated salt solution, are 0.13 and 1 weight-percent, respectively. These numbers show that the pure diffusion equation is not able to describe the phenomena and the chloride transport in water flux must also be considered. The chlorides penetrate into concrete during the wetting phases; in the following drying phases water evaporates from the surface and the dissolved salts are deposited in the form of crystals. Thus the chloride content in concrete continuously increases and is halted only by rainfall and seawater washing action. The environmental conditions in the numeric simulation were reproduced by assuming a step function for humidity and external solution concentration; the time period was 12 hr long, to represent the daily tidal cycle periods. The temperature was kept constant. The values of parameters used in the numerical analysis are summarized in Table 5.

Table 5—Values of parameters used in numerical simulation of chloride intrusion into concretes exposed to tidal cycles

Quantity	Concrete type		
	w/c = 0.4	w/c = 0.5	w/c = 0.6
ζ	0.7		
Humidity diffusion			
Porosity, %	11	13	15
D_h , m ² /sec	$1.0 \cdot 10^{-12}$	$5.0 \cdot 10^{-12}$	$2.5 \cdot 10^{-11}$
Initial humidity, h_i	100%		
Step-type boundary conditions	$h_{en,max} = 100\%$, $h_{en,min} = 0\%$ period = 12 hr		
Chloride diffusion			
Binding ratio γ	0.7		
k_{dil} , m/sec	$5.0 \cdot 10^{-9}$		
$D_{i,rif}$, m ² /sec	$1.0 \cdot 10^{-12}$		
Initial chloride concentration $C_{i,i}$, kg/m ³	0		
Step-type boundary conditions	$C_{en,max} = 13 \text{ kg/m}^3$, $C_{en,min} = 0$ period = 12 hr		

Fig. 10 shows the evolution of relative humidity, starting from the initial internal value of 100 percent, into a concrete exposed to tidal cycles for 10 years, with $D_{h,rif} = 2.5 \cdot 10^{-11}$ m²/sec. Fig. 11 represents the variation in time of total chloride concentration in a concrete of 15 percent porosity exposed to the conditions just listed. Finally, Fig. 12 compares the total chloride content in three different concretes (i.e., characterized by three different values of porosity) exposed for 10 years to tidal cycles; thus, the beneficial effect of a lower porosity in reducing chloride penetration is demonstrated. Avoiding the introduction of too many variables

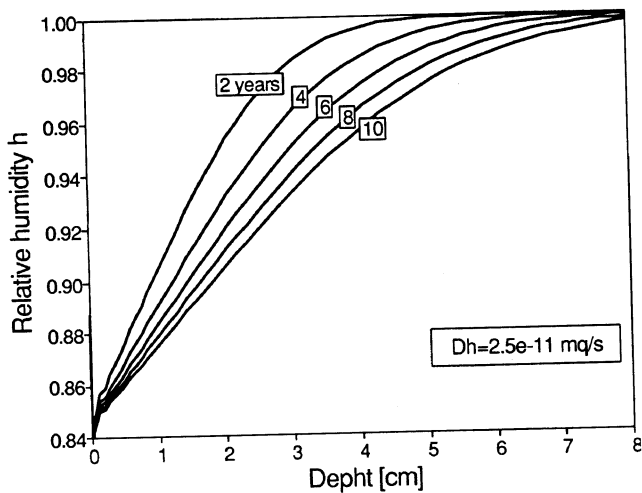


Fig 10—Evolution of relative humidity into concrete with $d_{h,rif} = 2.5 \cdot 10^{-11} m^2/sec$ exposed to tidal cycles for 12 years. Initial relative humidity $h_i = 100$ percent

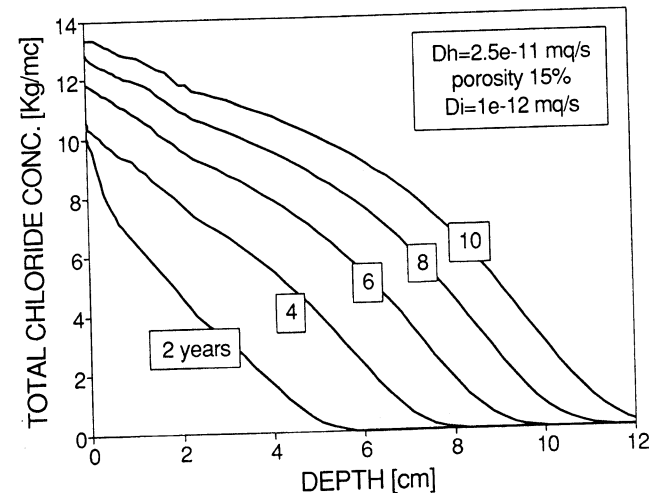


Fig 11—Diffusion kinetic of chloride ions into concrete exposed in tidal zone wetting-drying cycles for 10 years

makes the interpretation of numerical results easier; therefore, chloride diffusivity was kept constant for all the different concretes. The differences in the final ion contents are therefore due only to the different values of the concrete porosity and to the humidity diffusion coefficients used for the various concretes; this confirms the effectiveness of drying-wetting cycles in introducing chloride ions into concrete and the importance of concrete porosity in determining the total amount of chloride dragged by water flux.

CONCLUSIONS

Based on the results obtained and on comparisons with the experimental tests, the following conclusions can be drawn:

- The relationships used in describing the dependence of the chloride diffusion coefficient on the material parameters and the internal humidity and temperature appear to be adequate.
- Eq. (29) is able to simulate the exposure conditions of concrete structures to marine atmosphere.

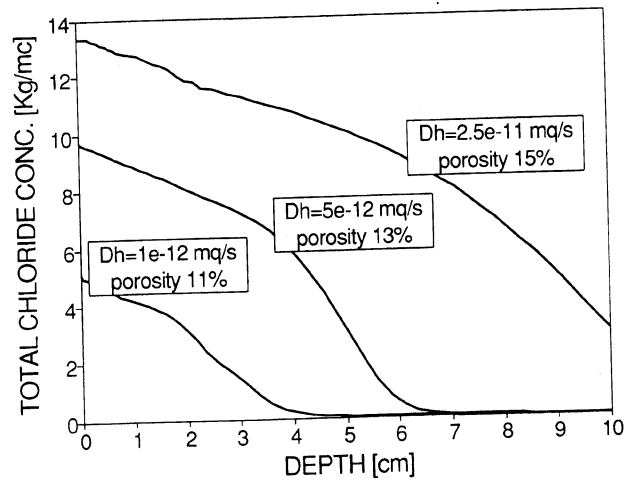


Fig 12—Comparison of different profiles of total chloride concentration obtained in concretes with porosity w_{sat} of 11, 13, and 15 percent after 4 years' exposure

- The ionic diffusion into partially saturated concrete was effectively reproduced.
- Eq. (21) permits a good agreement with experimental measurements. Permeable inflow of sea water during the wetting phase of wet/dry cycling causes a far greater ingress of chlorides than is caused by ionic diffusion alone. Thus, when porosity and humidity diffusion coefficients increase, a strong rise of the chloride content and of the penetration depths can be observed (Fig. 12).

The concordance of the model with the experimental results confirms the reliability and the effectiveness of the proposed numerical model. For a better definition of the parameter values used in the numerical tests, further comparisons with experimental data are needed. It is hoped that this work will lead to formulation of a simulation method of greater general applicability attainment of a more detailed understanding of the mechanism of chloride diffusion in partially saturated concrete.

CONVERSION FACTORS

1 kg = 2.2046 lb
1 m = 3.2808 ft
1 m/sec = 3.2808 ft/sec
1 m ² /sec = 10.7636 ft ² /sec
1/m ² ·sec = 0.09291 1/ft ² ·sec
1 kg/m ³ = 0.06242 lb/ft ³
1 kg/m ² ·sec = 0.2048 lb/(ft ² ·sec)
1 N = 0.2248 lb-force
1 J = 0.7375 ft-lb force
1 W = J/sec = 0.7375 ft-lb force/sec
T _C = (T _F - 32)/1.8

REFERENCES

1. Arya, C., and Newman, J. B., "Assessment of Four Methods of Determining the Free Chloride Content of Concrete," *Materials and Structures, Research and Testing* (RILEM, Paris), V. 23, 1990, pp. 319-330.
2. Arya, C.; Buenfeld, N. R.; and Newman, J. B., "Assessment of Simple Methods of Determining the Free Chloride Ion Content of Cement Paste," *Cement and Concrete Research*, V. 17, No. 6, 1987, pp. 907-918.

3. Hausmann, D. A., "Steel Corrosion in Concrete," *Materials Protection*, 1967, pp. 19-23.
4. Gouda, "Corrosion and Corrosion Inhibition of Reinforcing Steel Immersed in Alkaline Solutions," *British Corrosion Journal*, V. 5, 1970, pp. 198-203.
5. Beaudoin, J. J.; Ramachandran, V. S.; and Feldman, R. F., "Interaction of Chloride and C-S-H," *Cement and Concrete Research*, V. 20, No. 6, 1990, pp. 875-883.
6. Ramachandran, V. S.; Seeley, R. C.; and Polomark, G. M., "Free and Combined Chloride in Hydrating Cement and Cement Components," *Matériaux et Constructions*, V. 17, No. 100, 1984, pp. 285-289.
7. Tritthart, J., "Chloride Binding in Cement. II. Influence of the Hydroxide Concentration in the Pore Solution of Hardened Cement Paste on Chloride Binding," *Cement and Concrete Research*, V. 19, No. 5, 1989, pp. 683-691.
8. Neville, A. M., *Properties of Concrete*, 3rd Edition, Pitman Publishing Ltd., London, 1981, pp. 383-385.
9. Atkinson, A., and Nickerson A. K., "Diffusion of Ions through Water-Saturated Cement," *Journal of Material Science*, V. 19, 1984, pp. 3068-3078.
10. Collepardi, M.; Marciallis, A.; and Turriziani, R., "Penetration of De-icing Agents in Cement Pastes," *Industria Italiana del Cemento*, V. 69, 1972, pp. 143-150.
11. Collepardi, M.; Marciallis, A.; and Turriziani, R., "Cinetica di Penetrazione degli Ioni Cloruro nel Calcestruzzo (Kinetic of Penetration of Chloride Ions into Concrete)," *Industria Italiana del Cemento*, V. 4, Oct.-Dec. 1970, pp. 157-164.
12. Page, C. L.; Short, N. R.; and El Tarras, A., "Diffusion of Chloride Ions in Hardened Cement Paste," *Cement and Concrete Research*, V. 11, No. 3, 1981, pp. 395-406.
13. Byfors, K., "Influence of Silica Fume and Flyash on Chloride Diffusion and pH Values in Cement Paste," *Cement and Concrete Research*, V. 17, No. 1, 1987, pp. 115-130.
14. Detwiler, R. J.; Kjellsen, K. O.; and Gjørsv, O. E., "Resistance to Chloride Intrusion of Concrete Cured at Different Temperatures," *ACI Materials Journal*, V. 89, No. 1, Jan.-Feb. 1991, pp. 19-24.
15. Collepardi, M.; Marciallis, A.; and Turriziani, R., "Penetration of Chloride Ions in Cement Pastes and in Concretes," *Journal of the American Ceramic Society*, V. 55, No. 10, Oct. 1972, pp. 534-535.
16. Bazant, Z. P., and Najjar, L. J., "Nonlinear Water Diffusion in Non-Saturated Concrete," *Materials and Structures, Research and Testing (RILEM, Paris)*, V. 5, No. 25, 1972, pp. 3-20.
17. Mangat, P. S., and Gurusamy, K., "Chloride Diffusion in Steel Fibre Reinforced Concrete Containing PFA," *Cement and Concrete Research*, V. 17, No. 4, 1987, pp. 640-650.
18. Bamforth, P.B., and Pocock, D.C., "Minimising the Risk of Chloride Induced Corrosion by Selection of Concreting Materials," *Congress on Corrosion of Reinforcement in Concrete*, Elsevier Applied Science, London, 1989.
19. Bazant, Z. P., and Thonguthai, W., "Pore Pressure and Drying of Concrete at High Temperature," *Journal of Engineering Mechanics, ASCE*, V. 104, No. EM5, Oct. 1978, pp. 1059-1079.
20. Bazant, Z. P., and Najjar, L. J., "Drying of Concrete as a Nonlinear Diffusion Problem," *Cement and Concrete Research*, V. 1, 1971, pp. 461-473.
21. Masuda, Y., "Penetration mechanism of chloride ion into concrete," *Proceedings, RILEM 1st International Congress: From Materials Science to Materials Engineering (Versailles, 1987)*, Chapman and Hall, London, pp. 935-942.
22. Zienkiewicz, O. C., and Taylor, R. L., *Finite Element Method*, Fourth ed., V. 1, McGraw-Hill, 1989.
23. Hughes, T. J. R., *Finite Element Method*, Prentice-Hall, 1987.
24. Collepardi, M., and Biagini, S., "Effect of Water/Cement Ratio, Pozzolanic Addition and Curing Time of Chloride Penetration into Concrete," *ERMCO 89*, 1989.
25. Jaegermann, C., "Effect of Water-Cement Ratio and Curing on Chloride Penetration into Concrete Exposed to Mediterranean Sea Climate," *ACI Materials Journal*, V. 87, No. 4, July-Aug. 1990, pp. 333-339.
26. Uji, K.; Matsuoka, Y.; and Maruya, T., "Formulation of an Equation for Surface Chloride Content of Concrete due to Permeation of Chloride," *Congress on Corrosion of Reinforcement in Concrete*, Elsevier Applied Science, London 1989.